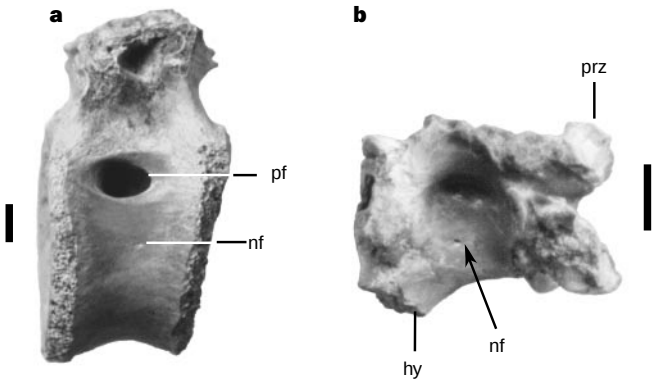

Figure 3 Thoracic vertebrae of **a**, dromaeosaurid theropod (AMNH 21893) and **b**, *Baptornis advenus* (AMNH 5101) in lateral view, showing the relative size difference between a pneumatic foramen (pf) as seen in the dromaeosaur and a non-pneumatic nutrient foramen (nf) present in *Baptornis*. *Baptornis* is a Cretaceous diving bird with apneumatic vertebrae. hy, hypapophysis; prz, prezygapophysis. Scale bars, 5 mm.

at the end of the tail. Most living birds have pneumatic cervical and thoracic vertebrae[15], and some, such as the turkey (*Meleagris*) and the ostrich (*Struthio*), exhibit pneumatization of the synsacral and free caudal vertebrae as well.

Identification of pneumatic foramina in *Archaeopteryx* links the evidence for axial pneumaticity seen in non-avialan theropods with the pneumatic features of Aves. According to present theories of bird origins[16], this phylogenetic continuity shows the homology of these structures. Although pneumatic postcranial bones are known in advanced pterosaurs[17] and sauropod dinosaurs[18], phylogenetic hypotheses[16,19,20] indicate that these incidences of postcranial pneumatic invasion occurred separately from that in theropods. Under these phylogenetic schemes, the distribution of vertebral pneumatization within Theropoda supports the proposed relationship of birds to theropods. This character distribution also shows that although axial pneumaticity may lighten the skeleton, its evolution cannot be considered to be an adaptation for flight *per se*.

A flow-through lung is unique to birds among extant vertebrates. This remarkable lung is distinctive for its associated system of air sacs, diverticula of which often invade the postcranial skeleton. The presence of pneumatic foramina in the vertebrae of many non-avialan and avialan theropods indicates that at least one of the components of the avian air-sac lung system, the cervical air sacs, was already in place in non-avialan theropods. In chickens (*Gallus*), the synsacral vertebrae are pneumatized by the abdominal air sacs[21], whereas in turkeys the cervical air sac extends all the way to the free coccygeal vertebrae[21]. It is impossible at present to determine which of these two air sacs is responsible for invading this part of the vertebral column in non-bird theropods with pneumatic sacral vertebrae, but it is possible that abdominal air sacs were present in these taxa. Clavicular air sacs are only positively known in Aves, although a large pneumatic foramen occurs on a single enantiornithine humerus (L. Chiappe, personal communication). Certain air sacs rarely (abdominal) or possibly never (thoracic) invade the skeleton in living birds[10], and their presence therefore remains enigmatic in stem avialans and more primitive theropods.

The evidence for components of the avian respiratory apparatus in non-avialan theropods raises questions about a claim that non-avialan theropods and Avialae have different accessory ventilatory mechanisms[22], the former having a hepatic-piston pump and the latter an air-sac system. The proposed presence of a hepatic-piston pump in non-avialan theropods is based on a preservational artefact (P. Currie, personal communication). Furthermore, the predictions of this hypothesis regarding the distribution of extreme opisthopuby among non-avialan and basal avialan theropods has not been supported by some fossil discoveries[14,23]. □

Received 29 January; accepted 7 July 1998.

1. Owen, R. On the *Archaeopteryx* of von Meyer, with a description of a new long tailed species from the lithographic stone of Solenhofen [sic]. *Phil. Trans.* **153,** 33–47 (1864).
2. Vogt, C. *Archaeopteryx macrura*, an intermediate form between birds and reptiles. *Ibis* **4,** 434–456 (1890).
3. Lambrecht, L. *Handbuch der Palaeornithologie* 1024 (Gebrüder Borntraeger, Berlin, 1933).
4. De Beer, Sir G. *Archaeopteryx lithographica* (Brit. Mus. Nat. Hist., London, 1954).
5. Bühler, P. in *Papers in Avian Paleontology Honoring Pierce Brodkorb* Science Ser. 36 (ed. Campbell, K. E. Jr) (Los Angeles County Mus., Los Angeles, 1992).
6. Martin, L. D. in *Origins of the Higher Groups of Tetrapods, Controversy amd Consensus* (eds Schultze, H.-P. & Trueb, L.) 485–540 (Cornell Univ. Press, Ithaca, 1991).
7. Müller B. The air-sacs of the pigeon. *Smithson. Misc. Coll.* **50,** 365–414 (1908).
8. Wellnhofer, P. Das fünfte Skelettexemplar von *Archaeopteryx*. *Palaeontograph. A* **147,** 169–216 (1974).
9. Ostrom, J. H. *Archaeopteryx* and the origins of birds. *Biol. J. Linn. Soc.* **8,** 91–182 (1976).
10. King, A. S. Structural and functional aspects of the avian lungs and air sacs. *Int. Rev. Gen. Exp. Zool.* **2,** 171–267 (1966).
11. Britt, B. B. *Pneumatic Postcranial Bones in Dinosaurs and Other Archosaurs.* Thesis, Univ. Calgary (1993).
12. Hogg, D. A. The development of pneumatisation in the postcranial skeleton of the domestic fowl. *J. Anat.* **139,** 105–113 (1984).
13. Britt, B. B. in *Encyclopedia of Dinosaurs* (eds Currie, P.C. & Padian, K.) 590–598 (Academic, San Diego, 1997).
14. Forster, C. A., Sampson, S. D., Chiappe, L. M. & Krause, D. W. The theropod ancestry of birds: new evidence from the Late Cretaceous of Madagascar. *Science* **279,** 1915–1919 (1998).
15. Boas, J. E. V. Studien über den Hals des Vögel. *Kgl. Danske Vidensk. Selsk. Skrifter* **9,** 101–222 (1929).
16. Gauthier, J. Saurischian monophyly and the origin of birds. *California Acad. Sci. Mem.* **8,** 1–55 (1986).
17. Wild, R. Die Flugsaurier (Reptilia, Pterosauria) aus der Oberen Trias von Cene bei Bergamo, Italien. *Boll. Soc. Paleont. Ital.* **17,** 176–256 (1978).
18. McIntosh, J. S. in *The Dinosauria* (eds Weishampel, D. B., Dodson, P. & Osmólska, H.) 345–401 (Univ. California Press, Berkeley, 1990).
19. Sereno, P. C. Basal archosaurs: phylogenetic relationships and functional implications. *Soc. Vertebr. Paleont. Mem.* **22,** 1–53 (1991).
20. Juul, L. The phylogeny of basal archosaurs. *Palaeont. Afr.* **31,** 1–38 (1994).
21. King, A. S. in *The Anatomy of the Domestic Animals* (ed. Getty, R.) 1883–1918 (W. B. Saunders, Philadelphia, 1975).
22. Ruben, J. A., Jones, T. D., Geist, N. R. & Jaap Hillenius, W. Lung structure and ventilation in theropods and early birds. *Science* **278,** 1267–1270 (1997).
23. Norell, M. A. & Makovicky, P. J. Important features of the dromaeosaur skeleton: information from a new specimen. *Am. Mus. Nov.* **3215,** 1–28 (1997).
24. Bonde, N. in *The Continental Jurassic* (ed. Morales, M.) 193–199 (Mus. North. Arizona Bull. 60, Flagstaff, 1996).

Acknowledgements. We thank the curatorial staffs of the American Museum of Natural History, British Museum of Natural History, Humboldt Museum für Naturkunde, Jura-Museum Eichstätt and Yale Peabody Museum for access to their specimens; and L. Barretti, M. Ellison and A. Gishlick for assistance with the production of the figures. This work was supported by the Royal Tyrrell Museum and the University of Calgary (B.B.B.), the Danish Research Academy and the AMNH (P.J.M.), an NSF grant and a travel grant from the Geraldine Lindsay Fund of the California Academy of Sciences (to J.G.), and a travel grant from the Geological Institute, Copenhagen University (to N.B.).

Correspondence and requests for materials should be addressed to P.J.M. (e-mail: pmako@amnh.org).

Object-based attention in the primary visual cortex of the macaque monkey

Pieter R. Roelfsema, Victor A. F. Lamme & Henk Spekreijse

Graduate School Neurosciences Amsterdam, Laboratory of Medical Physics, and the Netherlands Ophthalmic Research Institute (KNAW), Department of Visual System Analysis, Academic Medical Center (UvA), PO Box 12141, 1100 AC Amsterdam, The Netherlands

Typical natural visual scenes contain many objects, which need to be segregated from each other and from the background. Present theories subdivide the processes responsible for this segregation into a pre-attentive and attentive system[1,2]. The pre-attentive system segregates image regions that 'pop out' rapidly and in parallel across the visual field. In the primary visual cortex, responses to pre-attentively selected image regions are enhanced[3–5]. When objects do not segregate automatically from the rest of the image, the time-consuming attentive system is recruited. Here we investigate whether attentive selection is also associated with a modulation of firing rates in area V1 of the brain in monkeys trained to perform a curve-tracing task[6,7]. Neuronal responses to the various segments of a target curve

were simultaneously enhanced relative to responses evoked by a distractor curve, even if the two curves crossed each other. This indicates that object-based attention is associated with a response enhancement at the earliest level of the visual cortical processing hierarchy.

Visual attention has been suggested to act like a spotlight[8] or zoom lens[9] that is directed successively to image regions of interest. Neurons in extrastriate areas exhibit enhanced firing rates if attention is directed to the image location to which they respond[10–15]. Whether attentive rate modulation also occurs in the primary visual cortex is more controversial. Motter[15] demonstrated that visual attention is associated with a substantial enhancement of firing rates in area V1, but other studies have reported weaker[16] or marginal effects[12,17,18]. Attentive selection cannot be based entirely on the spatial position of a spotlight, however, because it can also be directed to one of two overlapping objects[19,20]. To select all features of an object in these situations, attention should be guided by perceptual grouping criteria such as connectedness and collinearity[21,22]. Because neurons in area V1 are sensitive for collinear arrangements of contour segments[23–25], we hypothesized that early visual areas might contribute to attentive selection. Activity in early visual areas might also enhance the spatial resolution of the selection process, which is important if components of different objects are close together.

Two monkeys were trained to perform a curve-tracing task[6,7]. In each trial the animals had to fixate a small circle in the middle of a computer screen (Fig. 1a). After 300 ms of fixation, two red circles and two curves appeared on the screen. One of the circles was connected to the fixation point through a curve, and served as target. The second circle was a distractor, and was not connected to the fixation point. After an additional delay of 600 ms the fixation point was extinguished, and an eye movement had to be made to the target circle. When the monkeys had learned the task, 40–50 multiunit electrodes were chronically implanted in the primary visual cortex.

Figure 1b, c illustrates the location of the receptive field of a recording site in area V1 relative to the visual stimuli. For the first stimulus (Fig. 1b) the receptive field was on the target curve, which connected the fixation point to the target circle. A small change in the stimulus close to the fixation point switched the identity of target and distractor (Fig. 1c) and, accordingly, the receptive field was on the distractor curve. The activity of the neurons was modulated by the difference between stimuli, although the location of the difference was far from the receptive field. The firing rate was highest when the receptive field was on the target curve (Fig. 1d). An analysis of the distributions of firing rates in single trials indicated that this rate enhancement was highly significant (*U*-test, $P < 10^{-6}$) (Fig. 1e).

A comparable enhancement of responses to the target curve was observed for the majority of recording sites in area V1. For all sites ($N = 45$), a modulation index was computed, which was defined as the ratio between rate enhancement (or reduction) and the average firing rate (see Methods). The distribution of modulation indices was shifted to positive values ($P < 0.0005$, sign-test), and had a median of 0.27 (Fig. 1f). This indicates that most cells in area V1 fire more action potentials if their receptive field is on the curve from the fixation point to the target.

To determine the latency of enhancement, responses at all recording sites with a significant rate enhancement ($P < 0.05$ and a positive modulation index, $N = 27$) were normalized to the peak response and averaged (see Methods) (Fig. 1g). The latency was defined as the first of three successive 10-ms bins with a significant difference between the two conditions ($P < 0.05$, paired *t*-test). At the population level, the latency was 235 ms, but in some individual cases it occurred slightly earlier (Fig. 1d). The visual response had a latency of 35 ms and preceded the rate enhancement by 200 ms. These results indicate that, whereas the early activity of a neuron in area V1 signals features of the contour segment inside the classical receptive field, later response components are influenced from remote locations. By the time of the response enhancement, transients evoked by the appearance of the stimulus have vanished from area V1 (Fig. 1g), which justifies computation of the strength of modulation during the ensuing episode of sustained firing.

The monkeys maintained visual fixation within a square window

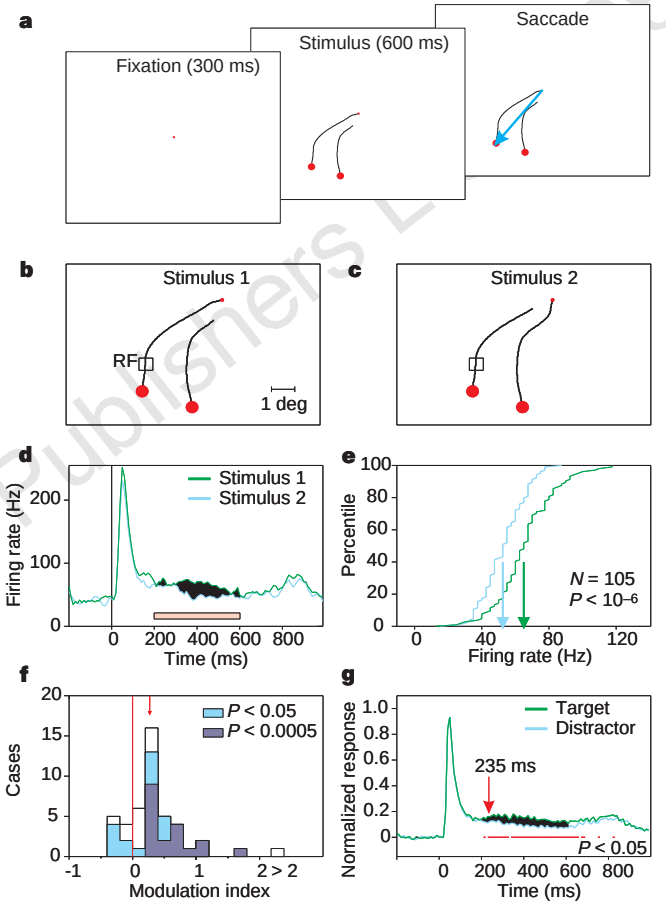

Figure 1 Response enhancement in area V1 during curve tracing. **a**, Sequence of images on the computer monitor during a single trial. Fixation had to be maintained until the fixation point disappeared, 600 ms after stimulus presentation. **b**, **c**, The rectangle shows the location of the receptive field (RF) of a group of neurons in area V1 relative to the stimuli. In **b** the receptive field was on the path from the fixation point to the target and in **c** it was not. **d**, Responses to the two stimuli. Green curve, response to stimulus 1. Blue curve, response to stimulus 2. The black area emphasizes the difference between the responses to the two stimuli during the computational window. Pink bar, computational window used for the analysis of firing rates in single trials. **e**, Distributions of firing rates in a window from 200 to 600 ms after stimulus onset, evoked by stimulus 1 (receptive field on path, green curve) and stimulus 2 (receptive field not on path, blue curve). The monkey performed 105 trials with both stimuli. The arrows indicate the medians of the two distributions that were significantly different (*U*-test, $P < 10^{-6}$). **f**, Distribution of the modulation index of all recording sites ($N = 45$). A positive modulation index indicates an enhanced response to the target curve (see Methods). Cases for which the difference between conditions was significant ($P < 0.05$, *U*-test) are shown in light blue, and highly significant cases are shown in dark blue ($P < 0.0005$). The arrow indicates the median (0.27). **g**, The latency of rate enhancement was estimated by averaging normalized responses at recording sites with a significantly positive modulation index ($P < 0.05$). Green curve, average response when the receptive field was on the target curve. Blue curve, average response when the receptive field was on the distracting curve. Red bars indicate 10-ms bins in which the difference between responses reached statistical significance (paired *t*-test, $P < 0.05$). Arrow, latency of response enhancement.

that was less than or equal to 1° × 1°. Nevertheless, microsaccades (small eye movements around the fixation point) occurred. A systematic difference in the pattern of microsaccades between stimuli could cause a modulation of firing rates, because it would be associated with a systematic shift of curves relative to the receptive fields. A stratification procedure was used to exclude this possibility. First, trials in which a microsaccade occurred within a window from 300 to 460 ms after stimulus onset were excluded from analysis (Fig. 2a). For the remaining trials of both stimulus conditions, distributions of eye positions were computed (Fig. 2b). Subsequently, the number of trials in each eye-position bin (0.2° × 0.2°) was made equal by removing excess trials in one or other condition. After this stratification procedure, firing rates were recalculated in a window from 400 to 500 ms after stimulus onset. This shorter window also excludes contributions of transient responses evoked by microsaccades occurring slightly before 300 ms. Figure 2c illustrates the effect of stratification on the distribution of firing rates at the recording site of Fig. 1. Exclusion of trials and the use of a shorter temporal window reduced the significance of the difference between conditions, but the magnitude of the modulation index was virtually unaltered, for the illustrated recording site ($P < 0.02$, U-test) and also at the population level (median = 0.28; $P < 0.005$, sign test) (Fig. 2d). Thus, rate enhancement is not caused by a systematic difference in visual fixation between the two stimulus conditions.

Rate enhancement was not restricted to neuronal responses to a specific segment of the target curve. Figure 3 illustrates an experiment in which simultaneous recordings were obtained from three groups of neurons, which responded to different segments of a single curve. When the respective receptive fields were on the target curve, responses at all recording sites were enhanced simultaneously. This demonstrates that the representation of the entire target curve 'lights up' in area V1 during this task.

Unlike response modulations observed in previous studies[3–5,23–25], the rate enhancement during curve tracing cannot be attributed to a pre-attentive mechanism, because the monkeys had to select one of two equally salient curves. Results from psychophysical studies are also inconsistent with pre-attentive processing in curve-tracing tasks, because reaction times exhibit an approximately linear dependence on the length of curve that should be traced[6,7]. We therefore conjecture that rate enhancement during curve tracing is due to attentive selection and that the latency of enhancement provides a measure for the time required to direct attention to the curve segment inside the receptive field.

Treisman and co-workers (for example, ref. 1) have suggested that focal attention needs to be directed to a visual object to integrate its various attributes into a coherent object representation. The curve-tracing task would have been solved as soon as visual attention had grouped contour segments into a coherent representation of the target curve, because this would identify the correct eye-movement target. However, in many of the stimuli used, it was virtually impossible for a circular spotlight to enclose the entire target curve while avoiding the distractor curve (Figs 1, 3). Nevertheless, responses to the various segments of the target curve were enhanced simultaneously, which suggests that object-based attention[19,22] is involved in curve tracing.

The case for the involvement of object-based attention would be strengthened if a selective enhancement of responses to the target curve were also to occur if the two curves were spatially overlapping. We therefore investigated activity in V1 by using a slightly modified

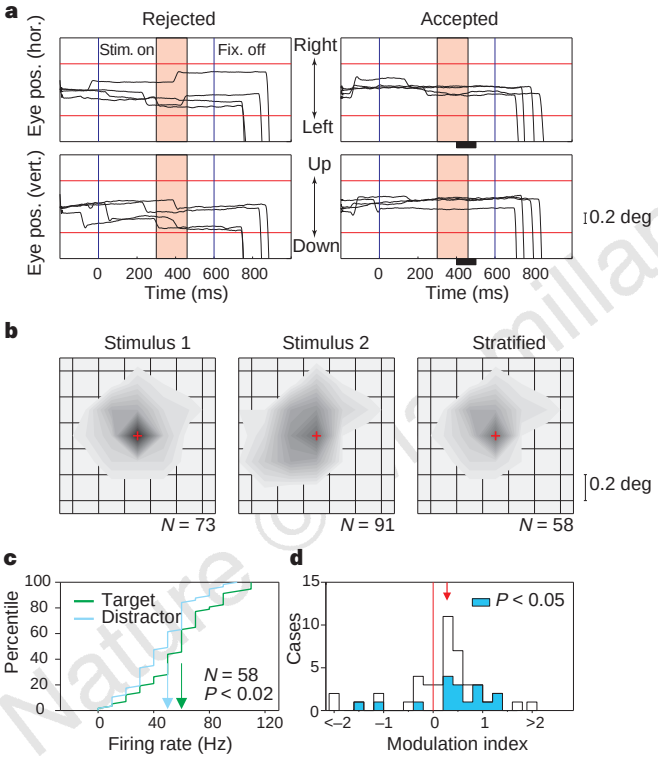

Figure 2 Rate enhancement is not caused by differences in fixation behaviour between stimulus conditions. **a**, Recordings of eye position during curve tracing. Upper panels, horizontal eye position. Lower panels, vertical eye position. Eye positions were determined for each trial in a window from 300 to 460 ms after stimulus onset (pink region). Eye position is only well defined for trials without a microsaccade in this window (right). Trials with a microsaccade in this window (left) were excluded from analysis. Red lines indicate the borders of the fixation window. Black rectangles below the abscissa indicate the time window used for computation of the firing rate distributions. **b**, Distribution of eye positions (0.2° × 0.2° bins) for the experiment shown in Fig. 1. Left, eye positions in trials with stimulus 1 ($N = 73$, after removal of trials with a microsaccade). Middle, eye positions for stimulus 2 ($N = 91$). Right, the stratified distribution of eye positions ($N = 58$) was obtained by removing excess trials in every bin. Red cross, location of fixation point. **c**, Distributions of firing rates at the same recording site as in Fig. 1 for the subset of trials obtained by stratification. Green curve, firing rates when the receptive field was on the target curve. Blue curve, firing rates when the receptive field was on the distractor curve. The arrows indicate the medians of the two distributions, which differed significantly (U-test, $P < 0.02$). **d**, Distribution of modulation indices after stratification ($N = 45$). Significant cases are shown in blue ($P < 0.05$, U-test). The arrow indicates the median modulation index (0.28).

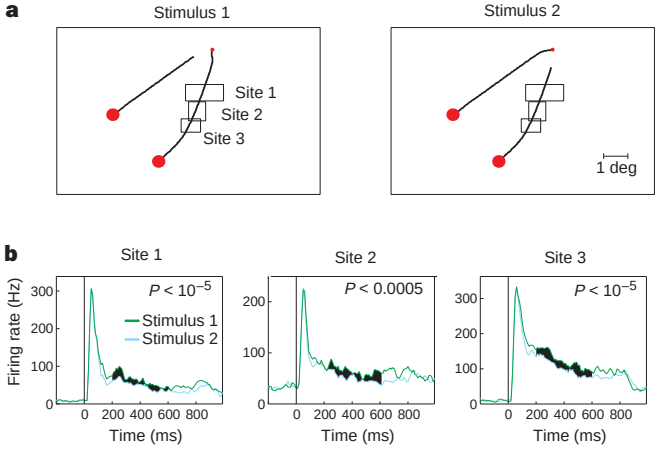

Figure 3 Simultaneous enhancement of responses to various segments of a single curve. **a**, Rectangles show the location of receptive fields at three recording sites from which simultaneous recordings were obtained. Receptive fields were all on the target curve for stimulus 1 (left), and on the distracting curve for stimulus 2 (right). **b**, Responses at the recording sites were simultaneously enhanced when the receptive fields were on the target curve.

task in which the target curve could cross the distractor curve. An additional location of stimulus variation, the 'switch-box', was introduced (inset in Fig. 4a, b). The two curves could intersect each other in the switch-box or stay separate. Figure 4 illustrates the location of the receptive fields of five simultaneously recorded groups of V1 neurons relative to the stimuli. When the two curves were non-intersecting (Fig. 4a), firing rates were enhanced significantly (yellow receptive fields; $P < 0.05$, difference between stimulus I and II) at recording sites that had their receptive field on the target curve, which is in accordance with the results of Figs 1 and 3. Notably, even if the two curves crossed each other, responses to the various segments of the target curve were simultaneously enhanced (Fig. 4b; yellow receptive fields). This enhancement was significant at four of the five recording sites ($P < 0.05$, difference between stimulus III and IV).

Cells at recording site 2 had their receptive field on the proximal curve segment, between the fixation point and the location at which an intersection could occur. Response enhancement at site 2 occurred for stimulus II and IV, although these stimuli were associated with different saccade targets (Fig. 4a–c). This indicates that rate enhancement does not depend solely on the location of fixation point and the planned eye movement, but rather on the position of the entire target curve. The population response of all recording sites with a receptive field on the proximal segment ($N = 15$) corroborates this result, and is shown in Fig. 4e. On average, responses were enhanced if the receptive field was on the target curve, for stimuli with (modulation index = 0.35; paired t-test, $P < 0.005$) and without (modulation index = 0.18; paired t-test, $P < 0.005$) an intersection.

The receptive field of neurons at recording site 3 was on the distal curve segment, between the switch-box and the circular targets. Response enhancement at this site occurred for stimulus I and IV (Fig. 4a, b, d). Thus, if there was no intersection, the response at recording site 3 was strongest if the fixation point was connected to the upper proximal segment, but this dependence was reversed in the presence of an intersection. This indicates that the response enhancement is not a simple sensory effect, caused by the presence of an additional contour segment at a specific location in the visual field. The population response of all recording sites with a receptive field on the distal segment ($N = 23$) confirms these results

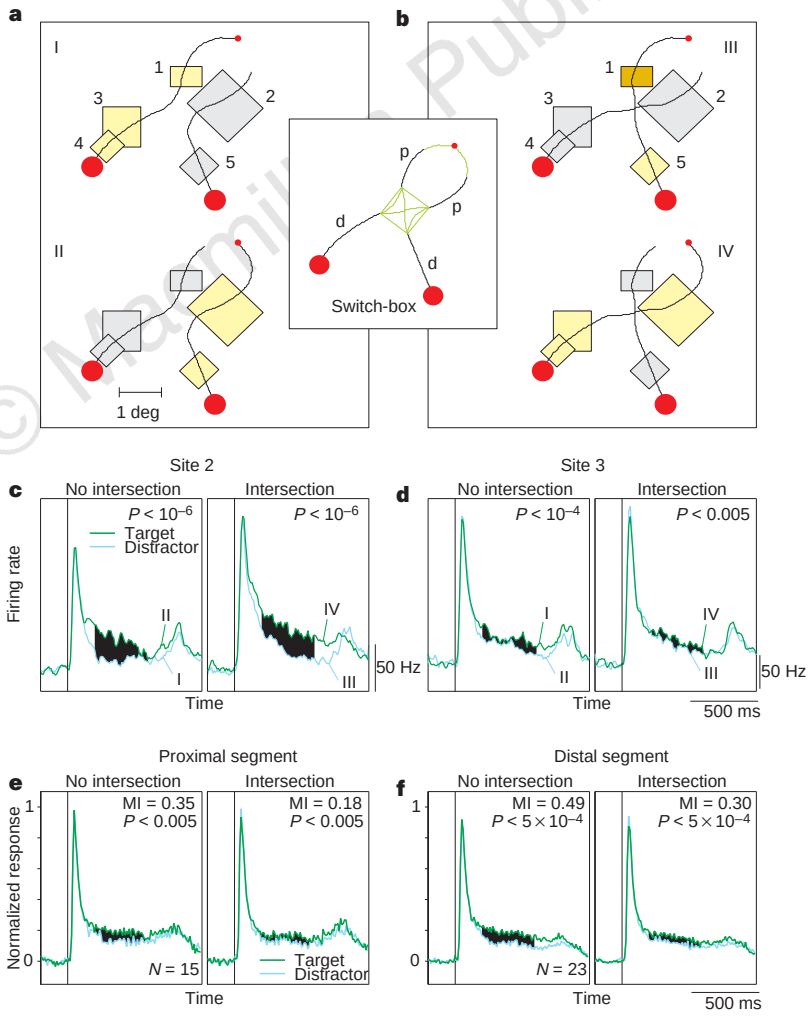

Figure 4 Response enhancement to stimuli in which the target and distractor curve could intersect each other. **a**, **b**, Complementary stimuli with (**b**) or without (**a**) an intersection. Rectangles show the receptive fields at five recording sites. Receptive fields in bright yellow are from recording sites at which responses to the target curve were significantly enhanced ($P < 0.05$; comparison between stimulus I and II, and between III and IV). The response enhancement at recording site 1 to stimulus III did not reach statistical significance (darkish yellow). Inset, design of the stimuli. Green contour segments varied between stimuli, black contour segments were identical. The green square indicates the switch-box. p, proximal curve segment. d, distal curve segment. **c**, **d**, Responses to complementary stimuli at recording site 2 (**c**) and recording site 3 (**d**). Responses to the target curve are shown in green, and responses to the distractor curve in blue. **e**, **f**, Responses pooled across all recording sites with a receptive field on the proximal curve segment (**e**), and distal curve segment (**f**). N, number of recording sites. The modulation indices (MI) refer to the medians of the MI distributions across recording sites.

(Fig. 4f). Responses were stronger, on average, if the receptive field was on the target curve, both for stimuli without an intersection (modulation index = 0.49; paired t-test, $P < 5 \times 10^{-4}$), as well as for stimuli with an intersection (modulation index = 0.30; paired t-test, $P < 5 \times 10^{-4}$). The population responses of Fig. 4e, f provide additional evidence against the possibility that response modulation is caused by a purely sensory effect related to the difference between stimuli close to the fixation point. The proximal curve segment was closest to the fixation point, but modulation was strongest for neurons with a receptive field on the distal curve segment.

In conclusion, neurons that respond to segments of an entire target curve simultaneously exhibit an enhanced firing rate, even if this curve crosses a second, irrelevant curve. This strongly suggests that rate modulations in area V1 provide a correlate of object-based attention. To label responses to one of the curves selectively, the distribution of the rate enhancement should depend on perceptual grouping criteria such as collinearity and connectedness. Horizontal connections in area V1 predominantly interconnect neurons that prefer collinear line elements and have closely spaced receptive fields[26,27]. These connections might be involved in the propagation of attentive rate modulations to neurons that respond to the various segments of a single curve. The high degree of positional specificity of V1 neurons (small receptive fields) might be essential for the selectivity of such a process in situations in which different curves come into close proximity. □

Methods

Curve-tracing task. Experiments were performed with two macaque monkeys. Monkeys were seated in a primate chair with the head restrained at a distance of 0.75 m from a computer monitor (resolution 1024 × 768, frame rate 70 Hz). The eye position was measured by using a double magnetic induction technique[28]. A trial was started as soon as the monkey's eye position was within a 1° × 1° (or 0.8° × 0.8°) square window centred on the fixation point (0.2° diameter). After an interval of 300 ms, the targets and curves were shown (Fig. 1a), but the monkey had to maintain fixation. The target and fixation point were red, and the curves white (luminance 85 cd m^{-2}) on a black background (luminance 1.5 cd m^{-2}). After an additional 600 ms the fixation point was extinguished, and the monkey made an eye movement to one of the targets. Eye movements to the target that was connected to the fixation point were rewarded with apple juice.

Surgical procedures. The monkeys underwent two operations under general anaesthesia. Anaesthesia was induced with ketamine (15 mg kg^{-1} injected intramuscularly) and was maintained after intubation by ventilation with a mixture of 70% N_2O and 30% O_2, supplemented with 0.8% isoflurane, fentanyl (0.005 mg kg^{-1} intravenously) and midazolam (0.5 mg kg^{-1} h^{-1} intravenously). In the first operation a head holder was implanted. In addition, a gold-plated copper ring was implanted under the conjunctiva of one eye for the measurement of eye position[28]. In the second operation 40–50 Teflon-coated platinum–iridium wires (diameter 25 μm, impedance 0.4–0.8 MΩ at 100 Hz) were implanted chronically in area V1. The tips of the wires were positioned 1–2 mm below the cortical surface. Therefore our sample is relatively devoid of recordings in the upper cortical layers. The animals recovered for at least 21 days before training was resumed and data collection was initiated. All procedures complied with the NIH Guide for Care and Use of Laboratory Animals (National Institute of Health, Bethesda, Maryland), and were approved by the institutional animal care and use committee of the Royal Netherlands Academy of Arts and Sciences.

Recording and data analysis. The eye position was recorded in every trial with a sampling rate between 0.5 and 1 kHz, and microsaccades were detected offline by an automated procedure that convoluted the eye position traces with a step function. For detection of multi-unit activity, signals were amplified, band-pass filtered and fed through a Schmitt trigger. Recordings with a sufficient signal-to-noise ratio were obtained from about 50% of the wires. For these recording sites, receptive field dimensions were determined with an automatic plotting procedure using moving light bars. Receptive field eccentricity ranged from 1° to 6°. Average receptive field size was 0.66 deg^2 (range 0.14–1.6 deg^2), which is well within the range of V1 receptive field dimensions obtained with single-cell recordings in awake monkeys[29], and with conventional multi-unit recordings in anaesthetized monkeys[30]. The significance of differences in response strength between stimuli was computed from the distributions of firing rates in single trials (Fig. 1e) using the Mann–Whitney U test. As a measure of the strength of response enhancement, a modulation index was computed in a computational window from 200 to 600 ms (Fig. 1f), or from 400 to 500 ms (Fig. 2d) after stimulus onset. The modulation index was defined as the difference in response strength normalized to the average: $(T - D)/([T + D]/2)$, where T and D are responses to the target and distractor curve, respectively, after subtraction of the spontaneous firing rate. The median modulation index for stimuli without intersections was 0.27, which corresponds to a rate enhancement by 31% ($T/D = 1.31$). To compute the latency of rate enhancement, a population response was computed (Fig. 1g) from the normalized responses at recording sites with a significantly positive modulation index ($P < 0.05$, $N = 27$). To derive the normalization parameters, responses at each recording site (10 ms bins) were first averaged across the two conditions (on-path and off-path). From this average the peak response (R_p) and the spontaneous firing rate (F_s) were determined. Responses to both stimuli were divided by $(R_p - F_s)$, after subtraction of F_s. This normalization procedure would preserve a difference in the peak response between stimuli. Normalized responses were averaged across recording sites, and in each 10 ms bin a paired t-test was performed on the distributions of firing rates across recording sites. The latency of response enhancement was identical if responses from all recording sites ($N = 45$) were used for the computation of the population response (including non-significant cases, and cases with a negative modulation index). The population responses to stimuli with the switch box (Fig. 4e, f) were also computed using all cases.

Received 21 May; accepted 9 July 1998.

1. Treisman, A. M. & Gelade, G. A feature-integration theory of attention. *Cogn. Psychol.* **12,** 97–136 (1980).
2. Posner, M. I. & Presti, D. E. Selective attention and cognitive control. *Trends Neurosci.* **10,** 13–17 (1987).
3. Lamme, V. A. F. The neurophysiology of figure-ground segregation in primary visual cortex. *J. Neurosci.* **15,** 1605–1615 (1995).
4. Zipser, K., Lamme, V. A. F. & Schiller, P. H. Contextual modulation in primary visual cortex. *J. Neurosci.* **16,** 7376–7389 (1996).
5. Knierim, J. J. & Van Essen, D. C. Neuronal responses to static texture patterns in area V1 of the alert macaque monkey. *J. Neurophysiol.* **67,** 961–980 (1992).
6. Jolicoeur, P., Ullman, S. & MacKay, M. Curve tracing: a possible basic operation in the perception of spatial relations. *Mem Cognit.* **14,** 129-140 (1986).
7. Pringle, R. & Egeth, H. E. Mental curve tracing with elementary stimuli. *J. Exp. Psychol.: Hum. Percept. Perform.* **14,** 716–728 (1988).
8. Posner, M. I., Snyder, C. R. R. & Davidson, B. J. Attention and the detection of signals. *J. Exp. Psychol.: Gen.* **109,** 160–174 (1980).
9. Eriksen, C. W. & St. James, J. D. Visual attention within and around the field of focal attention: a zoom lens model. *Percept. Psychophys.* **40,** 225–240 (1986).
10. Mausell, J. H. R. The brain's visual world: representation of visual targets in cerebral cortex. *Science* **270,** 764–769 (1995).
11. Moran, J. & Desimone, R. Selective attention gates visual processing in the extrastriate cortex. *Science* **229,** 782–784 (1985).
12. Luck, S. J., Chelazzi, L., Hillyard, S. A. & Desimone, R. Neural mechanisms of spatial selective attention in areas V1, V2, and V4 of macaque visual cortex. *J. Neurophysiol.* **77,** 24–42 (1997).
13. Treue, S. & Maunsell, J. H. R. Attentional modulation of visual motion processing in cortical areas MT and MST. *Nature* **382,** 539–541 (1996).
14. Bushnell, M. C., Goldberg, M. E. & Robinson, D. L. Behavioral enhancement of visual responses in monkey cerebral cortex. I. Modulation in posterior parietal cortex related to selective visual attention. *J. Neurophysiol.* **46,** 755–772 (1981).
15. Motter, B. C. Focal attention produces spatially selective processing in visual cortical areas V1, V2, and V4 in the presence of competing stimuli. *J. Neurophysiol.* **70,** 909–919 (1993).
16. Press, W. A. & van Essen, D. C. Attentional modulation of neuronal responses in macaque area V1. *Soc. Neurosci. Abstr.* **23,** 1026 (1997).
17. Wurtz, R. H. & Mohler, C. W. Enhancement of visual responses in monkey striate cortex and frontal eye fields. *J. Neurophysiol.* **39,** 766–772 (1976).
18. Haenny, P. E. & Schiller, P. H. State dependent activity in monkey visual cortex. I. Single cell activity in V1 and V4 on visual tasks. *Exp. Brain Res.* **69,** 225–244 (1988).
19. Duncan, J. Selective attention and the organization of visual information. *J. Exp. Psychol.: Gen.* **113,** 501–517 (1984).
20. Kanwisher, N. & Driver, J. Objects, attributes, and visual attention: which what and where. *Curr. Dir. Psychol. Sci.* **1,** 26–31 (1997).
21. Rock, I. & Palmer, S. The legacy of Gestalt psychology. *Sci. Am.* **263**(6), 48–61 (1990).
22. Kramer, A. F. & Jacobson, A. Perceptual organization and focused attention: the role of objects and proximity in visual processing. *Percept. Psychophys.* **50,** 267–284 (1991).
23. Nelson, J. I. & Frost, B. J. Intracortical facilitation among co-oriented, co-axially aligned simple cells in cat striate cortex. *Exp. Brain Res.* **61,** 54–61 (1985).
24. Kapadia, M. K., Ito, M., Gilbert, C. D. & Westheimer, G. Improvement in visual sensitivity by changes in local context: parallel studies in human observers and in V1 of alert monkeys. *Neuron* **15,** 843–856 (1995).
25. Polat, U., Mizobe, K., Pettet, M. W., Kasamatsu, T. & Norcia, A. M. Collinear stimuli regulate visual responses depending on cell's contrast threshold. *Nature* **391,** 580–584 (1998).

26. Bosking, W. H., Zhang, Y., Schofield, B. & Fitzpatrick, D. Orientation selectivity and the arrangement of horizontal connections in tree shrew striate cortex. *J. Neurosci.* **15,** 2112–2127 (1997).
27. Schmidt, K. E., Goebel, R., Löwel, S. & Singer, W. The perceptual grouping criterion of colinearity is reflected by anisotropies of connections in the primary visual cortex. *Eur. J. Neurosci.* **9,** 1083–1089 (1997).
28. Bour, L. J., Van Gisbergen, J. A. M., Bruijns, J. & Ottes, F. P. The double magnetic induction method for measuring eye movement—results in monkey and man. *IEEE Trans. Biomed. Eng.* **31,** 419–427 (1984).
29. Snodderly, D. M. & Gur, M. Organizaton of striate cortex of alert, trained monkeys (*Macaca fascicularis*): ongoing activity, stimulus selectivity, and widths of receptive field activating regions. *J. Neurophysiol.* **74,** 2100–2125 (1995).
30. Gattass, R., Gross, C. G. & Sandell, J. H. Visual topography of V2 in the macaque. *J. Comp. Neurol.* **201,** 519–539 (1981).

Acknowledgements. We thank J. C. de Feiter and K. Brandsma for technical assistance. The research of P.R.R. and V.A.F.L. was funded by a fellowship from the Royal Netherlands Academy of Arts and Sciences.

Correspondence and requests for materials should be addressed to P.R.R. (e-mail: p.roelfsema@ioi.knaw.nl).

An analgesia circuit activated by cannabinoids

Ian D. Meng*, Barton H. Manning*, William J. Martin† & Howard L. Fields*‡

*Departments of * Neurology, † Anatomy and ‡ Physiology, and the W. M. Keck Foundation Center for Integrative Neuroscience, University of California, San Francisco, California 94143-0114, USA*

Although many anecdotal reports indicate that marijuana and its active constituent, delta-9-tetrahydrocannabinol (delta-9-THC), may reduce pain sensation[1,2], studies of humans have produced inconsistent results[3–6]. In animal studies, the apparent pain-suppressing effects of delta-9-THC and other cannabinoid drugs[7–12] are confounded by motor deficits[13,14]. Here we show that a brainstem circuit that contributes to the pain-suppressing effects of morphine[15] is also required for the analgesic effects of cannabinoids. Inactivation of the rostral ventromedial medulla (RVM) prevents the analgesia but not the motor deficits produced by systemically administered cannabinoids. Furthermore, cannabinoids produce analgesia by modulating RVM neuronal activity in a manner similar to, but pharmacologically dissociable from, that of morphine. We also show that endogenous cannabinoids tonically regulate pain thresholds in part through the modulation of RVM neuronal activity. These results show that analgesia produced by cannabinoids and opioids involves similar brainstem circuitry and that cannabinoids are indeed centrally acting analgesics with a new mechanism of action.

The discoveries of the CB1 and CB2 cannabinoid receptors[16,17] and of two putative endogenous ligands for the CBI receptor[18,19] and the development of a specific CB1-receptor antagonist (SR141716A) (ref. 20) have intensified interest in the function of endogenous cannabinoid systems. The CB2 receptor is located in peripheral tissues, whereas the CB1 receptor is present on neurons throughout the brain, including in several pain-modulating centres[21]. Projections from the RVM to the dorsal horn of the spinal cord are important for the production of analgesia originating from supraspinal sites[22]. The RVM, which includes the nucleus raphe magnus, the nucleus gigantocellularis pars alpha and the adjacent reticular formation, is essential for systemic opioid-induced analgesia[15], and may also be involved in cannabinoid analgesia, as microinjection of cannabinoid agonists into the RVM suppresses pain-related behaviours[23].

To determine the contribution of the RVM to analgesia produced by a systemically administered cannabinoid, we inactivated the RVM by microinjection of the $GABA_A$ (γ-aminobutyric acid subtype A) receptor agonist muscimol. Rats with physiological saline microinjected into the RVM showed significant increases in tail-flick latencies after intravenous administration of 0.125 mg kg^{-1} and 0.25 mg kg^{-1} doses of WIN55,212-2, a cannabinoid receptor agonist (Fig. 1a). In contrast, animals microinjected with muscimol (50 ng) in the RVM before the administration of WIN55,212-2 showed no increase in tail-flick latencies (Fig. 1b). Muscimol microinjection also produced significant hyperalgesia in animals treated with systemic vehicle as compared with control rats microinjected with saline (latency 3.29 ± 0.21 versus 4.73 ± 0.09 s; $P < 0.05$). These results indicate that the activity of neurons in the RVM is necessary

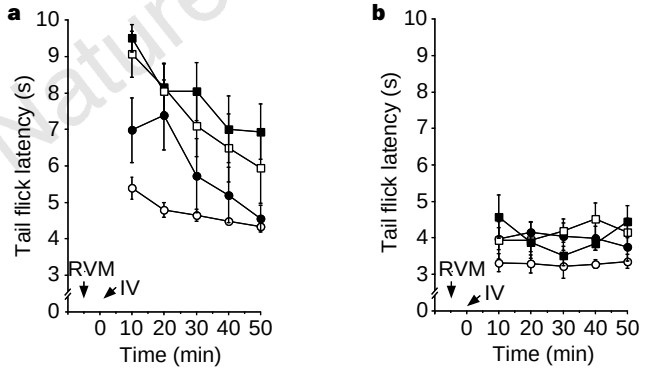

Figure 1 Inactivation of the RVM with microinjection of muscimol prevents the antinociception produced by the cannabinoid agonist WIN55,212-2. We measured tail-flick latencies in groups that received **a**, saline, or **b**, muscimol microinjections into the RVM before intravenous administration of vehicle (open circles); 0.0625 mg kg^{-1} WIN55,212-2 (filled circles); 0.125 mg kg^{-1} WIN55,212-2 (open squares); or 0.25 mg kg^{-1} WIN55,212-2 (filled squares). In saline-injected animals, consistent antinociception was achieved at the 0.125 and 0.25 mg kg^{-1} doses of WIN55,212-2 ($P < 0.01$; analysis of variance (ANOVA) followed by Fisher's least-significant difference (LSD) test). Muscimol-injected animals showed no difference in tail-flick latencies at any of the WIN55,212-2 doses ($P > 0.05$, ANOVA and Fisher's LSD test). Each value is the mean ± s.e.m.; tail-flick latencies represent the average of three trials; arrows indicate RVM and intravenous (IV) drug administration; $n = 6$ rats per group.

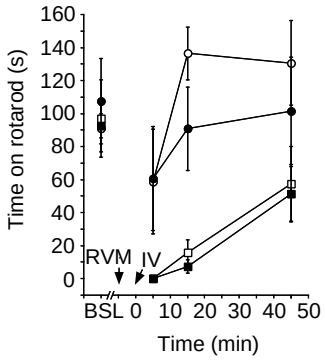

Figure 2 Cannabinoid-induced motor impairments are not affected by inactivation of the RVM with muscimol. Time on the rotarod treadmill (mean ± s.e.m.) was recorded from each of four groups (RVM microinjection/intravenous injection): open circles, saline/vehicle; filled circles, muscimol/vehicle; open squares, saline/WIN55,212-2; filled squares, muscimol/WIN55,212-2. Groups that received WIN55,212-2 (0.25 mg kg^{-1}) spent significantly less time on the rotarod as compared with vehicle-treated groups ($P < 0.01$; ANOVA and Fisher's LSD test). Injection of saline or muscimol into the RVM did not affect rotarod scores ($P > 0.05$; ANOVA). Baseline times (BSL) on the rotarod for each group before treatments were similar. Arrows indicate times of RVM and intravenous (IV) drug administration; $n = 5$ rats per group.